Water Research 164 (2019) 114885

Contents lists available at ScienceDirect

Water Research

journal homepage: www.elsevier.com/locate/watres

Selective adsorption of nitrate over chloride in microporous carbons

T.M. Mubita [a, b], J.E. Dykstra [a, *], P.M. Biesheuvel [b], A. van der Wal [a, c], S. Porada [b, d]

[a] Department of Environmental Technology, Wageningen University, Bornse Weilanden 9, 6708 WG Wageningen, the Netherlands
[b] Wetsus, European Centre of Excellence for Sustainable Water Technology, Oostergoweg 9, 8911 MA Leeuwarden, the Netherlands
[c] Evides Water Company, Schaardijk 150, 3063 NH Rotterdam, the Netherlands
[d] Soft Matter, Fluidics and Interfaces Group, Faculty of Science and Technology, University of Twente, Meander ME 314, 7500 AE Enschede, the Netherlands

ARTICLE INFO

Article history:
Received 2 May 2019
Received in revised form
4 July 2019
Accepted 18 July 2019
Available online 18 July 2019

Keywords:
Capacitive deionization
Ion electrosorption
Nitrate selectivity
Amphoteric donnan model

ABSTRACT

Activated carbon is the most common electrode material used in electrosorption processes such as water desalination with capacitive deionization (CDI). CDI is a cyclic process to remove ions from aqueous solutions by transferring charge from one electrode to another. When multiple salts are present in a solution, the removal of each ionic species can be different, resulting in selective ion separations. This ion selectivity is the result of combined effects, such as differences in the hydrated size and valence of the ions. In the present work, we study ion selectivity from salt mixtures with two different monovalent ions, chloride and nitrate. We run adsorption experiment in microporous carbons (i.e., without applying a voltage), as well as electrosorption experiments (i.e., based on applying a voltage between two carbon electrodes). Our results show that i) during adsorption and electrosorption, activated carbon removes much more nitrate than chloride; ii) at equilibrium, ion selectivity does not depend strongly on the composition of the water, but does depend on charging voltage in CDI; and iii) during electrosorption, ion selectivity is time-dependent. We modify the amphoteric Donnan model by including an additional affinity of nitrate to carbon. We find good agreement between our experimental results and the theory. Both show very high selectivity towards nitrate over chloride, $\beta_{NO_3^-/Cl^-}$ ~10, when no voltage is applied, or when the voltage is low. The selectivity gradually decreases with increasing charging voltage to $\beta_{NO_3^-/Cl^-}$ ~6 at $V_{ch} = 1.2$ V. Despite this decrease, the affinity-effect for nitrate continues to play an important role also at a high voltage. In general, we can conclude that our work provides new insights in the importance of carbon-ion interactions for electrochemical water desalination.

1. Introduction

Capacitive deionization (CDI) is a cyclic process to remove ions from aqueous solutions by electrostatic interactions with charged electrodes often made of porous carbon (Johnson and Newman, 1971; Tang et al., 2019). This cyclic process is performed by alternatingly charging and discharging the electrodes. During charging, ions are electrosorbed from the feed water and a desalinated stream is produced. The ions are temporarily stored in electrical double layers (EDLs), which are formed at the electrode-solution interface (Han et al., 2014; Porada et al., 2013; Wang et al., 2018). During discharge, ions are released from the electrodes and a concentrated stream is produced.

When multiple salts are present in the feed water, the adsorption of each ionic species can be different, resulting in selective removal of ions (Mossad and Zou, 2012; Suss, 2017; Tang et al., 2015). Several factors influence the ion adsorption capacity of individual ions from salt mixtures, including i) the material of the electrode, for instance an intercalation material (Singh et al., 2018), or porous carbons as we will focus on in this work; ii) for carbons, the pore characteristics, such as size (Hawks et al., 2019) and chemical surface charge (Han et al., 2014); iii) ion properties, such as ion valence (Hou and Huang, 2013), hydrated size (Gabelich et al., 2002), electronegativity (Sun et al., 2018), and the affinity of the ion to the carbon; and iv) operational conditions, such as charging and discharge voltage and initial ion concentration (Fig. 1a).

When ions have different valencies, it has been shown that a large selectivity can be obtained (Zhao et al., 2012b). However, for mixtures with two anions or two cations with the same valency (namely both monovalent), the results are more ambivalent. In some cases the selectivity is quite small (Dykstra et al., 2016a; Suss, 2017) and in some cases much more significant (Oyarzun et al.,

* Corresponding author
E-mail address: Jouke.Dykstra@wur.nl (J.E. Dykstra).

https://doi.org/10.1016/j.watres.2019.114885

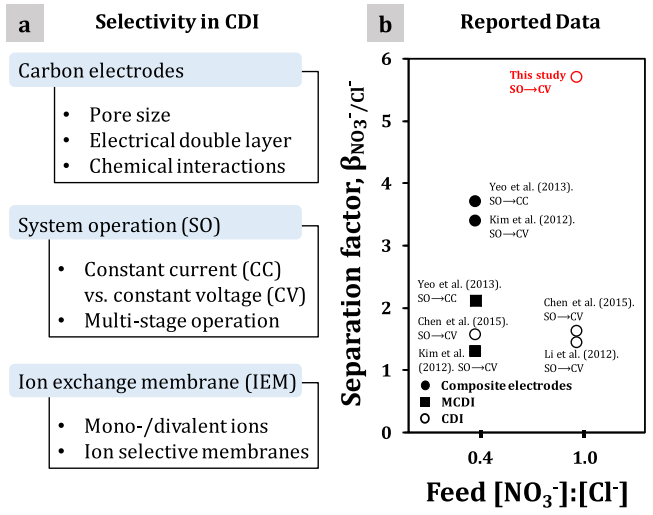

Fig. 1. a) Overview of several important aspects underlying preferential ion electrosorption in capacitive deionization with porous carbon electrodes; b) Experimental values of the separation factor between NO_3^- and Cl^- ($\beta_{NO_3^-/Cl^-}$) found in CDI and MCDI literature for constant current (CC) and constant voltage (CV) operation.

2018). It would seem that an affinity difference between the two ions, i.e., their non-electrostatic interaction with the carbon (micropores), can play a significant role when the carbon is uncharged (in an adsorption experiment) (Song et al., 2019), but most likely is overruled when two carbons are charged in a CDI-cell (electrosorption). In the second case, the electrostatic forces are strong (the voltage applied is many times the thermal voltage), and this is expected to overwhelm the affinity effect, which is voltage-independent. Our findings, as we will report below, are that indeed with increasing voltage the selectivity between two ions of the same valency, decreases when the charging voltage increases, in line with this expectation. However, as we also show, both experimentally and theoretically, the selectivity (β) for the ion pair NO_3^-/Cl^- remains very high, also at a voltage of $V_{ch} = 1.2$ V, where a value of $\beta_{NO_3^-/Cl^-}$ ~6 is found, dropping from a value ~10 in an adsorption experiment.

Before discussing our theoretical and experimental results in the next sections, we first present a literature overview of several experimental studies on selective ion removal from solutions containing two monovalent salts, or a mixture of one mono- and one divalent salt using electrodes made of carbon materials. Firstly, we describe studies on pore characteristics, then on ion properties, and lastly on system operation.

Early studies on preferential ion electrosorption in CDI focused on tuning the pore size distribution of the carbon material. Avraham et al. (2008) modified carbon fiber electrodes by chemical vapor deposition (CVD), and studied the effect of pore size distribution on the ion adsorption capacity using solutions containing one type of cation, which was either monovalent or divalent. Their results showed that, after CVD treatment, the capacity for divalent ions, such as calcium (Ca^{2+}) and magnesium (Mg^{2+}), decreased, whereas the capacity for monovalent ions, such as sodium (Na^+), did not change. They concluded that only ions that are smaller than the pore opening could enter the pores, which they called the ion sieving effect. In a follow-up study, electrodes modified by CVD were used to promote the electrosorption of nitrate (NO_3^-) over chloride (Cl^-) (Noked et al., 2009). The preference towards NO_3^- was attributed to the formation of narrow pore openings that allowed the passage of NO_3^-, with planar shape, and hindered the passage of Cl^-, with sphere-like shape; the so-called stereoselectivity effect was observed. Pore characteristics, as a factor determining ion selectivity, has also been studied by others. Han et al. (2014) indicated that ion selectivity largely depends on both pore-size characteristics and ion hydrated size. Eliad et al. (2001) concluded that, if the pores of the materials are considerably larger than the ion hydrated size, the adsorption capacity of the material is independent of the size and charge of the ions.

Apart from the pore size, ion properties influence selectivity in CDI. Gabelich et al. (2002) used carbon aerogel electrodes with a pore size larger than 4 nm to study the effect of valence, mass, and ion size on electrosorption capacity. Gabelich et al. found that ion valence was the main parameter determining ion selectivity. In solutions containing ions with different valences, selectivity is observed towards the ion with the highest valence. Zhao et al. (2012b) and Hou and Huang (2013) reported preferential electrosorption of Ca^{2+} over Na^+ ions, and Li et al. (2016) reported preferential electrosorption of sulfate (SO_4^{2-}) over NO_3^-. In Zhao et al. (2012b), experiments were conducted with an initial concentration of Na^+ that was five times higher than of Ca^{2+}. Initially, Na^+ ions were preferentially electrosorbed, but after some time, Ca^{2+} replaced the Na^+ ions. The separation factor of Ca^{2+} over Na^+ (Eq. (12)) for this experiment was ~7. When the adsorption time was extended from one to 5 h, the separation factor increased to ~25. Furthermore, Zhao et al. (2012b) also showed that the separation factor can be increased up to 300 when several desalination cycles are performed. This study illustrates that ion selectivity can be increased by adjusting the system operation.

For monovalent ions with different size, preferential ion electrosorption is often explained by a size-affinity trend, i.e., smaller ions are preferentially electrosorbed over larger ions (Dykstra et al., 2016a; Hou and Huang, 2013; Suss, 2017). For ions with the same valence and similar hydrated size, e.g., NO_3^- and Cl^-, ion selectivity cannot be related to ion size. Preferential separation of NO_3^- over Cl^- ions was studied by Chen et al. (2015) who reported that in the early stage of an adsorption step Cl^- ions were preferentially adsorbed in the EDLs, while at later stage Cl^- ions were replaced by NO_3^-. This result indicates that time dependent selectivity also occurs with mixtures of monovalent ions. Li et al. (2016) introduced the hydrated ratio, which is the ratio of the hydrated over the bare ion radius, to evaluate the preferential electrosorption of monovalent ions. This work reported selectivity towards anions with a higher hydrated ratio. Furthermore, Sun et al. (2018) tried to correlate selectivity with electronegativity. They found that ions with higher electronegativity are preferentially electrosorbed. Ion selectivity between monovalent ions has also been studied in modified carbon electrodes. Oyarzun et al. (2018) used carbon electrodes functionalized with quaternary amines (cathode) and benzene sulphonate (anode) to increase selectivity towards NO_3^- over Cl^-. Guyes et al. (2019) reported enhanced selectivity towards potassium ions with chemically oxidized cathodes.

The aforementioned studies are based on CDI with only carbon electrodes. Preferential electrosorption of ions can also be promoted with ion exchange membranes. Kim and Choi (2012) increased the selectivity towards NO_3^- by coating the anode surface of carbon electrodes with a polymeric solution containing NO_3^- selective ion exchange resins. With this approach, Kim et al. achieved a separation factor between NO_3^- and Cl^- ($\beta_{NO_3^-/Cl^-}$) of ~3.2, which was higher than the separation obtained with commercial ion exchange membranes (Fig. 1b). Preferential SO_4^{2-} removal was reported by Tang et al. (2017) using membrane capacitive deionization. Cation selectivity in intercalation materials for CDI, such as using Prussian Blue analogues, is reviewed by Singh et al. (2019). Lastly, new electrode materials have been developed to not only adsorb NO_3^- but also reduce it to nitrogen gas during electrode regeneration (Hu et al., 2018).

In the present work, we study selective removal of NO_3^- and Cl^- by porous carbons. We perform two different types of experiment: i) adsorption to study selective removal without electrically charging the carbon material, and ii) electrosorption with charging the carbon, i.e., CDI. The CDI experiments are performed as function of the NO_3^- over Cl^- ratio in the water and charging voltage. For both types of experiments, we find significant preferential removal of NO_3^- over Cl^-. We show that, in both cases, experimental data can be well described with the amphoteric Donnan model for ion adsorption in EDLs. In the model, we include a term to account for the affinity of the carbon surface for NO_3^-. We show that this affinity term leads to a high selectivity between the two ions in case of absence of a charging voltage (or a low voltage). Furthermore, we show that the affinity-effect remains important at a high voltage ($V_{ch} = 1.2$ V) where electrostatic effects also come to play a role.

2. Theory

To describe ion adsorption in the EDLs formed in microporous carbon materials, we use the amphoteric Donnan (amph-D) model. This model takes into account EDL overlap in sufficiently small micropores (smaller than the Debye length), which is typically the case for CDI with microporous carbons, and the model includes the presence of chemical charge on the surface of the carbon, i.e., lining the micropore regions (Arulrajan et al., 2019; Gao et al., 2016; Kim et al., 2019; Mubita et al., 2018). The amph-D model considers that there are two types of surface charge located in two different regions in the micropores: one region with acidic groups (region-A), and one region with basic groups (region-B). The two regions are expected to be near one another, well "mixed" throughout the electrode, but nevertheless each has its own distinct ionic composition, resulting from the difference in nearby surface charge.

Chemical interactions between ions and chemical groups present at the carbon surface can be included in the amph-D model, e.g., positively charged chemical groups at the surface, for which we use the general symbol B^+, can chemically bind ions, for example NO_3^-, according to the reaction $B^+ + NO_3^- \leftrightarrows B-NO_3$. This adsorption process can be modelled in equilibrium using a pK-constant, which describes the state of the equilibrium as function of the concentration of ionic species, and the number of free and occupied adsorption sites (Hiemstra et al. 1989, 1999). These chemical interactions between ions and chemical groups affect the adsorption of specific ions, as well as the chemical surface charge. Related is the pH-dependency of the acidic and basic groups as considered by Hemmatifar et al. (2017) in a model with acidic and basic groups, co-existing in the same micropore region (no separation in A- and B-regions).

Instead of considering the binding constants of ions with the different chemical groups, in the present work we use a simplified approach to describe chemical interactions by making use of a term,μ, that describes the affinity of the micropore for certain ions. This term is incorporated in the description of the ion concentration in the micropores ($c_{mi,i,j}$) according to the Boltzmann equilibrium. The resulting expression is

$$c_{mi,i,j} = c_{mA,i} \cdot \exp(-z_i \cdot \Delta\phi_{D,j} + \mu_i) \tag{1}$$

where subscript i refers to the ionic species, and subscript j to the micropore region, which can be either A or B. The concentration in the macropores is $c_{mA,i}$, z_i is the valence of the ion, and $\Delta\phi_{D,j}$ is the dimensionless Donnan potential. For all species, except for NO_3^-, we set μ to zero. Thus, only for NO_3^- we assume that the binding to chemical groups can be appreciable. For the other ions (Cl^- and K^+) we assume they do not have a significant chemical binding to the surface, and that they behave as inert species for which the normal Boltzmann distribution applies, i.e., Eq. (1) with $\mu = 0$. We use the same value of μ in both the A- and B-regions, i.e., the present model assumes the affinity effect for NO_3^- does not depend on the nature of the chemical charge.

In each region in the micropores, the amph-D model describes three types of charge: electronic charge in the carbon matrix (σ_{elec}) ionic charge in solution (σ_{ionic}) and chemical charge at the carbon surface (σ_{chem}). Overall, each region in the micropores is charge-neutral, and thus

$$\sigma_{elec,j} + \sigma_{chem,j} + \sigma_{ionic,j} = 0. \tag{2}$$

The acidic region has a negative value of σ_{chem}, whereas the basic region has a positive value of σ_{chem}. To calculate $\sigma_{ionic,j}$ in each region we use

$$\sigma_{ionic,j} = \sum_i z_i \cdot c_{mi,i,j}. \tag{3}$$

In the micropores, the ionic charge and electronic charge cannot come infinitely close; therefore, a dielectric layer is considered in between, which is called the Stern layer. The potential over this layer ($\Delta\phi_{S,j}$) is related to the Stern layer capacitance (C_S) and $\sigma_{elec,j}$ according to

$$\sigma_{elec,j} \cdot F = V_T \cdot \Delta\phi_{S,j} \cdot C_S \tag{4}$$

where F is the Faraday's constant, and V_T the thermal voltage, given by $V_T = RT/F$, with R the gas constant and T the temperature.

In each electrode (anode or cathode), the potential drop over the EDLs ($\Delta\phi_{EDL}$) is the sum of $\Delta\phi_D$ and $\Delta\phi_S$, and is equal for region A and B (Biesheuvel et al., 2015)

$$\Delta\phi_{EDL} = \Delta\phi_{D,A} + \Delta\phi_{S,A} = \Delta\phi_{D,B} + \Delta\phi_{S,B}. \tag{5}$$

In addition, for each electrode, we calculate the average value for σ_{elec} and σ_{ionic} using

$$\sigma_{elec} = \sum_{j=A,B} \alpha_j \cdot \sigma_{elec,j} \quad \text{, and} \quad \sigma_{ionic} = \sum_{j=A,B} \alpha_j \cdot \sigma_{ionic,j} \tag{6}$$

where α_j is the fraction of each region relative to the total micropore volume, $\upsilon_{mi,AC}$ (mL/g electrode).

At equilibrium (no transport of ions), the cell voltage is related to $\Delta\phi_{EDL}$ in the anode (an) and in the cathode (ca) by

$$\frac{V_{cell}}{V_T} = \Delta\phi_{EDLan} - \Delta\phi_{EDLca}. \tag{7}$$

The ion adsorption capacity of the electrodes (IAC) is calculated from the difference between the ion concentration in the micropore (c_i) at the end of the adsorption step (superscript "ads,end"), and the concentration at the end of the desorption step (superscript "des,end"), and when both electrodes have the same mass is given by (Biesheuvel et al., 2014)

$$IAC_i = \frac{1}{2} \cdot \upsilon_{mi,AC} \cdot \left(\left(c_i^{ads,end} - c_i^{des,end} \right)_{ca} + \left(c_i^{ads,end} - c_i^{des,end} \right)_{an} \right) \tag{8}$$

where

$$c_i = \sum_{j=A,B} \alpha_j \cdot c_{mi,i,j}. \tag{9}$$

The electrode charge (in C/g: defined per gram of two electrodes

combined) is given by

$$\Sigma_F = \tfrac{1}{2} \cdot F \cdot \upsilon_{mi,AC} \cdot \left| \sigma_{elec}^{ads,end} - \sigma_{elec}^{des,end} \right|. \quad (10)$$

Next, we define the charge efficiency for a mixture of monovalent ions as the ratio of the total number of ions adsorbed, divided by a factor 2, over the charge transferred,

$$\Lambda = \frac{F}{2} \cdot \frac{\sum_i IAC_i}{\Sigma_F} \quad (11)$$

where i runs over all adsorbed ions.

Finally, to describe ion selectivity in the EDLs, we use the separation factor (β), which is explained in detail by Suss (2017) and is expressed as

$$\beta_{1/2} = \frac{IAC_1}{IAC_2} \cdot \frac{c_{mA,2}}{c_{mA,1}} \quad (12)$$

where the subscripts 1 and 2 refer to the two different ionic species, e.g., NO_3^- and Cl^-.

The set of equations (1)–(12) describes ion adsorption in the micropores for a process that at the end of each step (charging step, discharge step) reaches equilibrium, i.e., there is no longer transport of ions into the micropores, and is valid irrespective of the valences of the participating ions (except Eq. (11)).

3. Experimental

3.1. Adsorption experiments

Batch experiments were conducted to study the adsorption of ions in activated carbon (AC) powder, which is equilibrated with a salt solution. A mass of 2 g of dry AC (YP-50F, Kuraray Chemical, Japan) were immersed in 20 mL of multi-ionic solutions containing either: i) one dissolved salt, either 20 mM KNO_3 or 20 mM KCl; or ii) salt mixtures with different NO_3^- to Cl^- concentration ratios, such as 1:2 and 2:1 (21 mM total ionic strength), and 1:3, 1:1, and 3:1 (20 mM total ionic strength). The solution was continuously stirred for 24 h, which is sufficiently long to reach equilibrium in the ion transport between bulk solution and micropores. After this time, the solution was filtered and the concentration of each ion in the filtrate was analyzed by ion chromatography (IC). The ion concentration in the micropores ($c_{mi,i}$) was calculated from the ion mass balance

$$V_{sol} \cdot c_{initial,i} = \upsilon_{mi,AC} \cdot m_{AC} \cdot c_{mi,i} + \left(V_{sol} - \upsilon_{mi,AC} \cdot m_{AC}\right) \cdot c_{final,i} \quad (13)$$

where V_{sol} is the volume of solution, m_{AC} the mass of AC, $\upsilon_{mi,AC}$ the AC micropore volume, $c_{initial,i}$ the initial concentration of ion i, and $c_{final,i}$ the concentration of ion i at the end of the adsorption experiment.

3.2. Electrosorption experiments

CDI experiments were conducted in a stack with four cells. Each cell consisted of two graphite current collectors, a pair of carbon electrodes (Materials & Methods, PACMM™ 203, Irvine, CA, electrode area = 33.8 cm^2) and a spacer channel (Glass fiber filter, cat No. AP2029325, Millipore, δ_{sp} ~250 μm) placed in between the electrodes, through which an aqueous solution flows. The electrodes used in the present study have been electrochemically characterized by other researchers (Oyarzun et al., 2018; Zhao et al., 2012a). The stack was ensembled as described by Porada et al. (2012) in which an aqueous solution flows in between the electrodes through the spacer channel. The aqueous solution with a total volume of 160 mL was pumped through the stack with a flow rate of 30 mL/min. The system was operated in batch-wise mode: the solution was pumped from the feed container into the stack, and the effluent of the stack was recirculated to the feed container. The charging voltage (V_{ch}) and discharge voltage (V_{dch}) were controlled and the current was measured using a potentiostat (Ivium Technologies, the Netherlands). For each experiment, we ran three cycles (charging/discharge) to achieve dynamic equilibrium, i.e., when the dynamic data of effluent concentration and current of a particular cycle is the same as of the previous cycle. Thereafter, the fourth cycle was performed, and we took samples from the feed container at different times during charging and discharge. The ion concentration in solution was measured by IC. With this concentration and the volume of solution, we obtain the mole of ions in solution. The difference between the mole of ions at the beginning of the electrosorption experiment and at equilibrium is the total ion adsorption. This total ion adsorption was divided by the total mass of electrodes to obtain IAC in mol/g. The half cycle time (HCT), which is the duration of each step (charging or discharge), was always 90 min, unless otherwise noted. We present an overview of experimental conditions in Table 1.

4. Results and discussion

4.1. Adsorption experiments: activated carbon is selective towards NO_3^-

Fig. 2 shows the NO_3^- and Cl^- concentration in the micropores of the carbon particles as function of the NO_3^- to Cl^- equilibrium concentration ratio in solution. Preferential NO_3^- adsorption is observed, even when the concentration of Cl^- is three times higher than that of NO_3^-. Experiments performed with single salt solutions (either NO_3^- or Cl^- in solution) showed that the concentration of Cl^- ions in the micropores is 34% lower than that of NO_3^-: $c_{mi,Cl^-} = 86$ mM and $c_{mi,NO_3^-} = 130$ mM. These results show that commercial activated carbon materials, which are often used to fabricate electrodes for CDI (Dykstra et al., 2016b; Hatzell et al., 2014; Reale and Smith, 2018), have an affinity that favors the adsorption of NO_3^- in carbon micropores.

Pore size and surface chemistry are affected by the fabrication and activation method of AC and play an important role on the adsorption capacity of AC (Chen and Wu, 2004; Li et al., 2002; Seredych et al., 2008). In the present work, we report data obtained with microporous AC: 80% of the total pore volume is due to pores with a size between 0.6 and 2 nm (Porada et al., 2013). These pores are larger than the hydrated size of the ions used in this study, and thus, are accessible for ions. Therefore, we consider that the surface chemistry, rather than the pore size, has an effect on the preferential adsorption of ions.

The surface chemistry of the AC is related to the presence of functional groups, which are: i) acidic groups, primarily oxygen containing groups, such as phenolic, carboxylic, and lactonic, and ii) basic groups, such as nitrogen containing functional groups, or π-electrons on the graphene layer (Boehm, 1994; Shafeeyan et al., 2010). Depending on the conditions, such as the pH and solvent characteristics, these functional groups can be dissociated or protonated, thereby inducing attractive or repulse interactions with the ions in solution (Sun et al., 2017). As the strength of the interactions between ions and functional groups is not the same for all ions, we observe an effect on the preferential adsorption of ions (Ota et al., 2013).

In Fig. 2, we also show four theory curves: two curves for NO_3^- and two for Cl^-. We used the affinity term (μ), which describes the

Table 1
Overview of electrosorption experimental conditions.

Experiment type	Initial salt concentration	Operational mode
Effect of the initial ion concentration (Fig. 3)	Concentration ratio of NO_3^- to Cl^- 1:2; 2:1 (total = 21 mM) 1:3; 1:1; 3:1 (total = 20 mM)	CV V_{ch} = 1.2 V V_{dch} = 0 V
Effect of the charging voltage (Fig. 4)	$[NO_3^-]$ = 10 mM $[Cl^-]$ = 10 mM	CV V_{ch} = 0.6; 0.8; 1.0; 1.2 V V_{dch} = 0 V
Preferential ion electrosorption (Fig. 5a)	$[NO_3^-]$ = 10 mM $[Cl^-]$ = 10 mM	CV V_{ch} = 1.2 V V_{dch} = 0 V
Ion displacement (Fig. 5b)	Step I: $[NO_3^-]$ = 20 mM* Step II: $[Cl^-]$ = 20 mM#	CV V_{ch} = 1.2 V, t_{ch} = 30 min CV V_{ch} = 1.2 V, t_{ch} = 90 min

CV = constant voltage; * first step: CV charging for 30 min, 20 mM KCl solution; # second step: addition of 20 mM KNO_3 while keeping V_{ch} = 1.2 V for t_{ch} = 90 min.

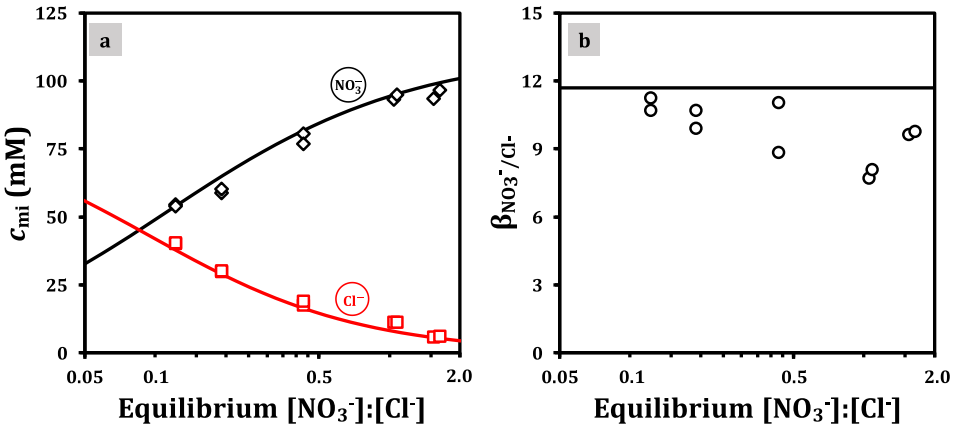

Fig. 2. Adsorption in uncharged carbon powder. a) Experimental data (symbols) and theoretical curves of the ion concentration in the micropores (c_{mi}) of activated carbon, and b) the separation factor ($\beta_{NO_3^-/Cl^-}$) both as function of equilibrium concentration ratio in solution, $[NO_3^-]:[Cl^-]$. In all calculations, we assumed that the volume of solution is 160 mL and that the total initial ionic strength was 20 mM, although in experiments with an initial concentration ratio of 2:1 and 1:2, the total initial ionic strength was 21 mM.

interaction between each ion in solution with the uncharged carbon material, as a fitting parameter. Theory describes our data very closely when the value of $\mu_{NO_3^-}$ is 2.46 (Table 2).

4.2. Effect of the initial ion concentration and charging voltage on ion selectivity in CDI

Fig. 3a and Fig. 3b show equilibrium electrosorption data of $\beta_{NO_3^-/Cl^-}$ and the ion adsorption capacity (IAC) as function of the NO_3^- to Cl^- concentration ratio in the feed solution. We observe that $\beta_{NO_3^-/Cl^-}$ increases with the NO_3^- to Cl^- concentration ratio in feed solution (Fig. 3a). In Fig. 3b, we see that with increasing initial NO_3^- to Cl^- concentration ratio, the difference between the concentration of NO_3^- and Cl^- in the micropores increases. Before equilibrium is reached, however, preferential ion electrosorption is determined by the initial concentration ratio: the ion with the highest concentration in solution was predominantly electrosorbed (data not shown).

Fig. 4a shows that $\beta_{NO_3^-/Cl^-}$ decreases with charging voltage, but the affinity-effect does not diminish much and continues to play an important role also at a high voltage. Charge and IAC increase with charging voltage (Fig. 4b and c). Fig. 4d shows that the charge efficiency is much lower than unity, which can be explained by the desorption of co-ions (ions with the same charge as the electrode)

Table 2
Parameters used in the theory to describe ion selectivity in the EDLs.

amph-D model			
$\sigma_{chem,A}$	Chemical surface charge - acidic region	- 0.26	M
$\sigma_{chem,B}$	Chemical surface charge - basic region	+0.26	M
$\upsilon_{mi,AC}$	Micropore volume carbon powder (adsorption)	0.82	mL/g
	Micropore volume electrode (electrosorption)	0.49	mL/g
C_S	Stern capacitance (adsorption)	145	F/mL
	Stern capacitance (electrosorption)	175	F/mL
$\mu_{NO_3^-}$	Affinity term for NO_3^- adsorption in micropores	2.46	
α_j	Fraction of region A and B relative to $\upsilon_{mi,AC}$	1/2	
R	Gas constant	8.314	J/mol/K
F	Faraday constant	96485	C/mol
T	Temperature	298	K

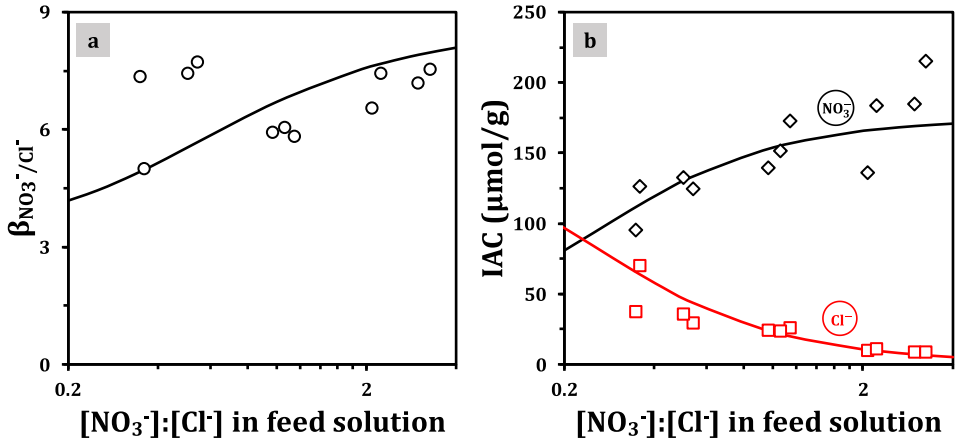

Fig. 3. Ion electrosorption in CDI (V_{ch} = 1.2 V). Data measured at equilibrium at different initial NO_3^- to Cl^- concentration ratio in solution. a) Separation factor; b) ion adsorption capacity per gram of both electrodes. Solid lines are the predictions of the numerical model.

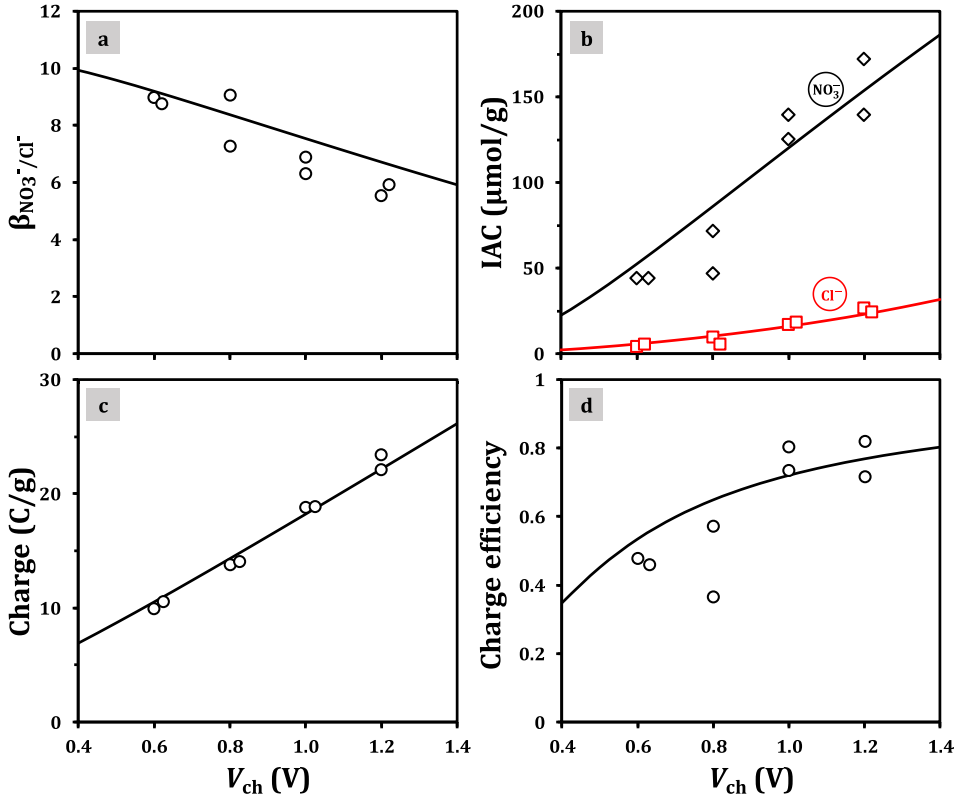

Fig. 4. Ion electrosorption in CDI. a) Separation factor; b) ion adsorption capacity per gram of both electrodes; c) charge; and d) charge efficiency, as function of the charging voltage (V_{ch}) Each plot shows two experimental data sets, both obtained at $c_{initial,NO_3^-} \sim 10$ mM and $c_{initial,Cl^-} \sim 10$ mM. Solid lines are the predictions of the numerical model.

from the carbon surface at the beginning of the charging step (Dykstra et al., 2016b; Hassanvand et al., 2018; Zhao et al., 2010).

To describe the experimental data in Figs. 3 and 4, we use the theory outlined in Section 2. For the calculations, values for parameters σ_{chem}, $\upsilon_{mi,AC}$, C_S, and μ_i are required. The parameter value for σ_{chem} was obtained from Biesheuvel (2015), while the other parameters were fitted (see Table 2). We find that both the adsorption and electrosorption data are theoretically described using the same value for μ_i. For the adsorption experiments, for which activated carbon powder was used, we found a micropore volume significantly higher than the micropore volume of the electrosorption experiments, for which electrodes were used. This finding is supported by previous work that showed that the micropore volume of activated carbon (Kuraray YP-50F) (0.67 mL/g AC) was significantly higher than the micropore volume of the electrode material per gram of dry activated carbon used for synthesis (0.56 mL/g AC) (Dykstra et al., 2016b).

4.3. Electrosorption of nitrate and chloride: ion selectivity is controlled by kinetics and equilibria

Next, we analyze the dynamics of preferential electrosorption (Table 1). Fig. 5a shows that the NO_3^- concentration continuously decreases for about 30 min until it reaches a constant value,

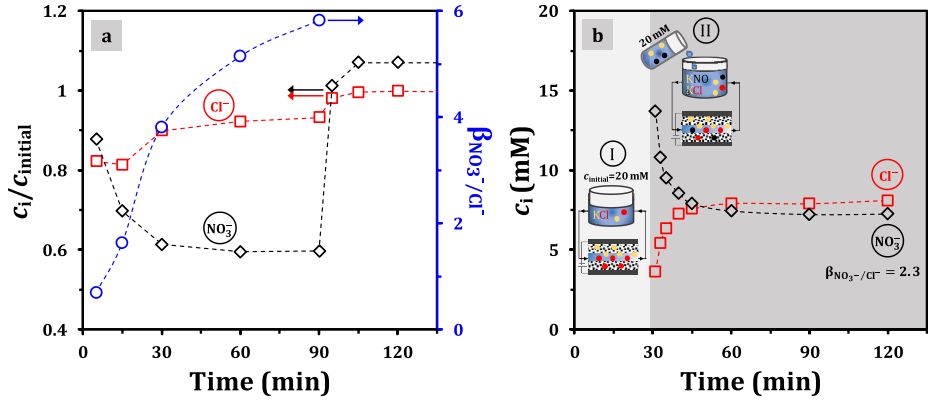

Figure 5. a) Anion concentration in solution and separation factor as a function of time; V_{ch} = 1.2 V; $c_{initial,NO_3^-} \sim 10$ mM and $c_{initial,Cl^-} \sim 10$ mM. b) Concentration of NO_3^- and Cl^- ions as function of time (ion displacement experiment). At step I, only Cl^- ions are electrosorbed for 30 min (NO_3^- ions were not present in feed solution). Thereafter, a 20 mM KNO_3 solution is added to the feed container (step II). Dashed lines serve to guide the eye.

whereas the Cl^- concentration decreases only for about 15 min. Thereafter, we observe an increase of the Cl^- concentration in solution, which means that NO_3^- ions gradually displace Cl^- ions. This phenomenon was previously reported by Chen et al. (2015) for the same mixture of ions.

According to Hassanvand et al. (2018), ion selectivity can be explained as a two-step phenomenon: the first step is controlled by ion kinetics and the second by adsorption equilibria. We will analyze both phenomena. To quantify ion selectivity, we use the separation factor ($\beta_{NO_3^-/Cl^-}$), which we show in Fig. 5a as function of time. Values of $\beta_{NO_3^-/Cl^-}$ higher than 1 indicate that NO_3^- ions are preferentially electrosorbed over Cl^- ions. As Fig. 5a shows, the separation factor increases over time, which indicates that preferential ion electrosorption is a time-dependent process. At the beginning of the charging step more Cl^- than NO_3^- is electrosorbed in the EDLs: $\beta_{NO_3^-/Cl^-} = 0.7$. At this stage, it is likely that ion selectivity is governed by ion transport to the micropores: the faster ion, in this case Cl^-, is preferentially electrosorbed (see diffusion coefficients of the ions in Table 3). As electrosorption progresses, $\beta_{NO_3^-/Cl^-}$ increases as a consequence of the displacement of Cl^- by NO_3^-. At equilibrium, $\beta_{NO_3^-/Cl^-}$ reaches a maximum value of ~6.0 at $V_{ch} = 1.2$ V.

Ions in aqueous solution are surrounded by layers of water molecules that form the hydration shell (Marcus, 2012). The ion hydration energy indicates how strong the ions hold these water molecules (Tansel, 2012). The structure of the hydration shell can suffer rearrangements (partial dehydration or complete loss of the water molecules) depending on the interaction of ions with the surface through which they flow (Collins, 1995; Epsztein et al., 2018). Ions with lower hydration energy can more easily rearrange their hydration shell compared to ions with higher hydration energy. It has been shown that ions need to strip off or deform their hydration shell to enter pores with smaller size than the ion hydrated size (Kalluri et al., 2013). The mean size of the pores contained in our electrodes is larger than the ion hydrated size. Thus, the pore size might not induce large perturbations in the hydration shell of NO_3^- and Cl^-, when these ions enter the pores. Therefore, structural changes on the hydration shell are probably not the main cause of preferential electrosorption of NO_3^-. Ion-carbon surface interactions may play a more important role in determining ion selectivity.

To support our findings of preferential adsorption of NO_3^- over Cl^- at equilibrium, we also conducted two-stage electrosorption experiments (Fig. 5b). In the first stage, we charged the cell to 1.2 V with only K^+ and Cl^- ions in solution. After 30 min, a 20 mM KNO_3 solution was added to the feed container (same volume as the KCl solution in the feed container, thus the resulting ion concentrations in the feed container are $[K^+] = 20$ mM, $[Cl^-] = 10$ mM, and $[NO_3^-] = 10$ mM), and the charging voltage was maintained for another 90 min. As Fig. 5a shows, Cl^- starts to desorb from the EDLs immediately after NO_3^- is added to the solution. We observe an increase in the Cl^- concentration, while the NO_3^- concentration decreases. Approximately 15 min after the addition of NO_3^-, we observe only minor concentration changes.

5. Conclusions

In this work, we present adsorption and electrosorption data for nitrate and chloride ions. At equilibrium, we observe preferential adsorption of nitrate over chloride in the micropores. Several factors can contribute to the preferential electrosorption of ions, such as the hydrated size of the ions and the interactions between the ions and the carbon surface. As the hydrated size of nitrate and chloride are equal, we conclude that the preferential adsorption of nitrate over chloride is due to chemical interactions between the ions and the carbon surface.

We also presented theory based on the amphoteric Donnan (amph-D) model to predict selectivity between nitrate and chloride in the micropores. The theory can be extended to describe preferential adsorption of other monovalent ions as well. Until now, the

Table 3
Physicochemical properties of the anions studied in the present work.

Ion	Ionic radius (Å) [a]	Hydrated radius (Å) [a]	Hydration energy (kJ/mol) [b]	Diffusion coefficient (10^{-9} m^2 s^{-1}) [c]
Cl^-	1.81	3.32	−381	2.03
NO_3^-	2.64	3.35	−314	1.90
K^+	1.33	3.31	−322	1.96

[a] Nightingale (1959).
[b] Smith (1977).
[c] Haynes (2012).

amph-D model has not been used to describe ion selectivity. We included an affinity term to describe the preferential adsorption of nitrate into the micropores. Although this affinity term is not associated to any particular property of the ion or micropore, it certainly describes the interaction between ions and the uncharged carbon particles. We acknowledge that this interaction is influenced by the surface chemistry and ion properties. Both theory and data underpin that a specific adsorption effect is not overruled by electrostatic phenomena.

Declaration of interest

The authors declare that they have no known competing financial interests or personal relationships that could have appeared to influence the work reported in this paper.

Acknowledgments

This work was performed in the cooperation framework of Wetsus, European Centre of Excellence for Sustainable Water Technology (www.wetsus.eu). Wetsus is co-funded by the Dutch Ministry of Economic Affairs and Climate Policy, the Northern Netherlands Provinces, the Province of Fryslân. This work is part of the Veni research programme with project number 15071, which is partly financed by the Dutch Research Council (NWO). The authors like to thank the participants of the research theme Capacitive Deionization for fruitful discussions and financial support.

References

Arulrajan, A.C., Ramasamy, D.L., Sillanpää, M., van der Wal, A., Biesheuvel, P.M., Porada, S., Dykstra, J.E., 2019. Exceptional water desalination performance with anion-selective electrodes. Adv. Mater. 31, 1806937.

Avraham, E., Yaniv, B., Soffer, A., Aurbach, D., 2008. Developing ion electro-adsorption stereoselectivity, by pore size adjustment with chemical vapor deposition onto active carbon fiber electrodes. Case of Ca2+/Na+ separation in water capacitive desalination. J. Phys. Chem. C 112, 7385–7389.

Biesheuvel, P.M., 2015. Activated Carbon Is an Electron-Conducting Amphoteric Ion Adsorbent. ARXIV 1509.06354.

Biesheuvel, P.M., Hamelers, H.V.M., Suss, M.E., 2015. Theory of water desalination by porous electrodes with immobile chemical charge. Colloid. Interface Sci. Commun. 9, 1–5.

Biesheuvel, P.M., Porada, S., Levi, M., Bazant, M.Z., 2014. Attractive forces in microporous carbon electrodes for capacitive deionization. J. Solid State Electrochem. 18, 1365–1376.

Boehm, H.P., 1994. Some aspects of the surface chemistry of carbon blacks and other carbons. Carbon 32, 759–769.

Chen, J.P., Wu, 2004. Acid/base-treated activated carbons: characterization of functional groups and metal adsorptive properties. Langmuir 20, 2233–2242.

Chen, Z., Zhang, H., Wu, C., Wang, Y., Li, W., 2015. A study of electrosorption selectivity of anions by activated carbon electrodes in capacitive deionization. Desalination 369, 46–50.

Collins, K., 1995. Sticky ions in biological systems. Proc. Natl. Acad. Sci. U.S.A. 92, 5553–5557.

Dykstra, J.E., Dijkstra, J., van der Wal, A., Hamelers, H.V.M., Porada, S., 2016a. On-line method to study dynamics of ion adsorption from mixtures of salts in capacitive deionization. Desalination 390, 47–52.

Dykstra, J.E., Zhao, R., Biesheuvel, P.M., van der Wal, A., 2016b. Resistance identification and rational process design in capacitive deionization. Water Res. 88, 358–370.

Eliad, L., Salitra, G., Soffer, A., Aurbach, D., 2001. Ion sieving effects in the electrical double layer of porous carbon electrodes: estimating effective ion size in electrolytic solutions. J. Phys. Chem. B 105, 6880–6887.

Epsztein, R., Shaulsky, E., Dizge, N., Warsinger, D.M., Elimelech, M., 2018. Role of ionic charge density in donnan exclusion of monovalent anions by nanofiltration. Environ. Sci. Technol. 52, 4108–4116.

Gabelich, C., Tran, T., Suffet, I., 2002. Electrosorption of inorganic salts from aqueous solution using carbon aerogels. Environ. Sci. Technol. 36, 3010–3019.

Gao, X., Porada, S., Omosebi, A., Liu, K.L., Biesheuvel, P.M., Landon, J., 2016. Complementary surface charge for enhanced capacitive deionization. Water Res. 92, 275–282.

Guyes, E.N., Malka, T., Suss, M.E., 2019. Enhancing the ion size-based selectivity of capacitive deionization electrodes. Environ. Sci. Technol. 53, 8447–8454.

Han, L., Karthikeyan, K.G., Anderson, M.A., Gregory, K.B., 2014. Exploring the impact of pore size distribution on the performance of carbon electrodes for capacitive deionization. J. Colloid Interface Sci. 430, 93–99.

Hassanvand, A., Chen, G.Q., Webley, P.A., Kentish, S.E., 2018. A comparison of multicomponent electrosorption in capacitive deionization and membrane capacitive deionization. Water Res. 131, 100–109.

Hatzell, M.C., Raju, M., Watson, V.J., Stack, A.G., van Duin, A.C.T., Logan, B.E., 2014. Effect of strong acid functional groups on electrode rise potential in capacitive mixing by double layer expansion. Environ. Sci. Technol. 48, 14041–14048.

Hawks, S.A., Cerón, M.R., Oyarzun, D.I., Pham, T.A., Zhan, C., Loeb, C.K., Mew, D., Deinhart, A., Wood, B.C., Santiago, J.G., Stadermann, M., Campbell, P.G., 2019. Using ultramicroporous carbon for the selective removal of nitrate with capacitive deionization. Environ. Sci. Technol. https://doi.org/10.1021/acs.est.9b01374.

Haynes, W.M., 2012. In: CRC Handbook of Chemistry and Physics, 93rd Edition. Taylor & Francis.

Hemmatifar, A., Oyarzun, D.I., Palko, J.W., Hawks, S.A., Stadermann, M., Santiago, J.G., 2017. Equilibria model for pH variations and ion adsorption in capacitive deionization electrodes. Water Res. 122, 387–397.

Hiemstra, T., Riemsdijk, W.H.v., Bolt, G.H., 1989. Multisite proton adsorption modeling at the solid/solution interface of (Hydr)oxides: a new approach. J. Colloid Interface Sci. 133, 91–104.

Hiemstra, T., Yong, H., Riemsdijk, W.H.v., 1999. Interfacial charging phenomena of aluminum (Hydr)oxides. Langmuir 15, 5942–5955.

Hou, C.-H., Huang, C.-Y., 2013. A comparative study of electrosorption selectivity of ions by activated carbon electrodes in capacitive deionization. Desalination 314, 124–129.

Hu, C., Dong, J., Wang, T., Liu, R., Liu, H., Qu, J., 2018. Nitrate electro-sorption/reduction in capacitive deionization using a novel Pd/NiAl-layered metal oxide film electrode. Chem. Eng. J. 335, 475–482.

Johnson, A.M., Newman, J., 1971. Desalting by means of porous carbon electrodes. J. Electrochem. Soc. 118, 510–517.

Kalluri, R.K., Biener, M.M., Suss, M.E., Merrill, M.D., Stadermann, M., Santiago, J.G., Baumann, T.F., Biener, J., Striolo, A., 2013. Unraveling the potential and pore-size dependent capacitance of slit-shaped graphitic carbon pores in aqueous electrolytes. Phys. Chem. Chem. Phys. 15, 2309.

Kim, M., Cerro, M.d., Hand, S., Cusick, R.D., 2019. Enhancing capacitive deionization performance with charged structural polysaccharide electrode binders. Water Res. 148, 388–397.

Kim, Y.J., Choi, J.H., 2012. Selective removal of nitrate ion using a novel composite carbon electrode in capacitive deionization. Water Res. 46, 6033–6039.

Li, L., Quinlivan, P.A., Knappe, D.R.U., 2002. Effects of activated carbon surface chemistry and pore structure on the adsorption of organic contaminants from aqueous solution. Carbon 40, 2085–2100.

Li, Y., Zhang, C., Jiang, Y., Wang, T.-J., Wang, H., 2016. Effects of the hydration ratio on the electrosorption selectivity of ions during capacitive deionization. Desalination 399, 171–177.

Marcus, Y., 2012. Ionic Interactions in Natural and Synthetic Macromolecules. John Wiley & Sons, Inc, pp. 1–33.

Mossad, M., Zou, L., 2012. A study of the capacitive deionisation performance under various operational conditions. J. Hazard Mater. 213–214, 491–497.

Mubita, T.M., Porada, S., Biesheuvel, P.M., van der Wal, A., Dykstra, J.E., 2018. Capacitive deionization with wire-shaped electrodes. Electrochim. Acta 270, 165–173.

Nightingale, E.R., 1959. Phenomenological theory of ion solvation. Effective radii of hydrated ions. J. Phys. Chem. 63, 1381–1387.

Noked, M., Avraham, E., Bohadana, Y., Soffer, A., Aurbach, D., 2009. Development of anion stereoselective, activated carbon molecular sieve electrodes prepared by chemical vapor deposition. J. Phys. Chem. C 113, 7316–7321.

Ota, K., Amano, Y., Aikawa, M., Machida, M., 2013. Removal of nitrate ions from water by activated carbons (ACs)—influence of surface chemistry of ACs and coexisting chloride and sulfate ions. Appl. Surf. Sci. 276, 838–842.

Oyarzun, D.I., Hemmatifar, A., Palko, J.W., Stadermann, M., Santiago, J.G., 2018. Ion selectivity in capacitive deionization with functionalized electrode: theory and experimental validation. Water Res. X 1, 100008.

Porada, S., Borchardt, L., Oschatz, M., Bryjak, M., Atchison, J.S., Keesman, K.J., Kaskel, S., Biesheuvel, P.M., Presser, V., 2013. Direct prediction of the desalination performance of porous carbon electrodes for capacitive deionization. Energy Environ. Sci. 6, 3700–3712.

Porada, S., Weinstein, L., Dash, R., van der Wal, A., Bryjak, M., Gogotsi, Y., Biesheuvel, P.M., 2012. Water desalination using capacitive deionization with microporous carbon electrodes. ACS Appl. Mater. Interfaces 4, 1194–1199.

Reale, E.R., Smith, K.C., 2018. Capacitive performance and tortuosity of activated carbon electrodes with macroscopic pores. J. Electrochem. Soc. 165, A1685–A1693.

Seredych, M., Hulicova-Jurcakova, D., Lu, G.Q., Bandosz, T.J., 2008. Surface functional groups of carbons and the effects of their chemical character, density and accessibility to ions on electrochemical performance. Carbon 46, 1475–1488.

Shafeeyan, M.S., Daud, W.M.A.W., Houshmand, A., Shamiri, A., 2010. A review on surface modification of activated carbon for carbon dioxide adsorption. J. Anal. Appl. Pyrolysis 89, 143–151.

Singh, K., Bouwmeester, H.J.M., de Smet, L.C.P.M., Bazant, M.Z., Biesheuvel, P.M., 2018. Theory of water desalination with intercalation materials. Phys. Rev. Appl. 9, 064036.

Singh, K., Porada, S., de Gier, H.D., Biesheuvel, P.M., de Smet, L.C.P.M., 2019. Timeline on the application of intercalation materials in capacitive deionization. Desalination 455, 115–134.

Smith, D.W., 1977. Ionic hydration enthalpies. J. Chem. Educ. 54, 540–542.
Song, J., Ma, J., Zhang, C., He, C., Waite, T.D., 2019. Implication of non-electrostatic contribution to deionization in flow-electrode CDI: case study of nitrate removal from contaminated source waters. Front. Chem. 7.
Sun, Z., Chai, L., Liu, M., Shu, Y., Li, Q., Wang, Y., Qiu, D., 2018. Effect of the electronegativity on the electrosorption selectivity of anions during capacitive deionization. Chemosphere 195, 282–290.
Sun, Z., Chai, L., Shu, Y., Li, Q., Liu, M., Qiu, D., 2017. Chemical bond between chloride ions and surface carboxyl groups on activated carbon. Colloid. Surf. Physicochem. Eng. Asp. 530, 53–59.
Suss, M.E., 2017. Size-based ion selectivity of micropore electric double layers in capacitive deionization electrodes. J. Electrochem. Soc. 164, E270–E275.
Tang, W., He, D., Zhang, C., Waite, T.D., 2017. Optimization of sulfate removal from brackish water by membrane capacitive deionization (MCDI). Water Res. 121, 302–310.
Tang, W., Kovalsky, P., He, D., Waite, T.D., 2015. Fluoride and nitrate removal from brackish groundwaters by batch-mode capacitive deionization. Water Res. 84, 342–349.
Tang, W., Liang, J., He, D., Gong, J., Tang, L., Liu, Z., Wang, D., Zeng, G., 2019. Various cell architectures of capacitive deionization: recent advances and future trends. Water Res. 150, 225–251.
Tansel, B., 2012. Significance of thermodynamic and physical characteristics on permeation of ions during membrane separation: hydrated radius, hydration free energy and viscous effects. Separ. Purif. Technol. 86, 119–126.
Wang, L., Biesheuvel, P.M., Lin, S., 2018. Reversible thermodynamic cycle analysis for capacitive deionization with modified Donnan model. J. Colloid Interface Sci. 512, 522–528.
Zhao, R., Biesheuvel, P.M., Miedema, H., Bruning, H., van der Wal, A., 2010. Charge efficiency: a functional tool to probe the double-layer structure inside of porous electrodes and application in the modeling of capacitive deionization. J. Phys. Chem. Lett. 1, 205–210.
Zhao, R., Biesheuvel, P.M., van der Wal, A., 2012a. Energy consumption and constant current operation in membrane capacitive deionization. Energy Environ. Sci. 5, 9520–9527.
Zhao, R., van Soestbergen, M., Rijnaarts, H.H.M., van der Wal, A., Bazant, M.Z., Biesheuvel, P.M., 2012b. Time-dependent ion selectivity in capacitive charging of porous electrodes. J. Colloid Interface Sci. 384, 38–44.